Magnetic Field Modeling Database Description

Haje Korth, Mikhail I. Sitnov, Grant K. Stephens
The Johns Hopkins University Applied Physics Laboratory
5 January 2018

Introduction

Magnetic field models of the Earth's magnetosphere have a wide range of research applications, and their complexity has increased substantially over past decades as the number and spatial distribution of observations in the magnetosphere multiplied. Magnetospheric magnetic field models are mathematical descriptions of the magnetic field source internal and external to the planet. For the Earth, the internal field is typically represented by the dynamo and the external field is generated by magnetospheric current systems flowing on the magnetopause boundary, in the magnetotail, in the ring current, and along magnetic field lines to the ionosphere. While the structure and equations differ between models, they all strive to contain the magnetospheric magnetic field within the magnetopause boundary, thus shielding the magnetospheric from the interplanetary magnetic field.

Generalized approaches to shielding arbitrary current systems at the magnetopause have been demonstrated, among others, for the terrestrial magnetosphere. To develop a magnetospheric magnetic field model, one must derive the magnetopause shape. One then solves the Chapman-Ferraro problem [*Chapman and Ferraro*, 1930] to derive the magnetopause current system that separates planetary and interplanetary magnetic fields. Given a magnetopause shape, the shielding magnetopause currents yield a net magnetic field at the magnetopause for which the component normal to the magnetopause, B_n, vanishes. Early models of the terrestrial magnetosphere [e.g., *Mead*, 1964] sought analytic solutions to this problem, which exist only for certain magnetopause shapes and magnetic field source distributions. Schulz and McNab [1987] generalized a technique to treat the magnetopause as a source surface [*Schatten et al.*, 1969] and determined the shielding field by minimizing the mean value of B_n on the magnetopause rather than requiring that it be precisely zero everywhere on this surface. Alternatively, a finite difference technique can be used to solve the Chapman-Ferraro problem numerically [*Toffoletto et al.*, 1994]. These approaches allow fitting of shielding fields to arbitrary current distributions in the magnetosphere and to arbitrary shapes of the magnetopause. The source-surface method has been adopted for a series of empirical models of the terrestrial magnetosphere [*Tsyganenko*, 1995; 2002a; b; *Tsyganenko and Sitnov*, 2005; 2007; *Sitnov et al.*, 2008; *Tsyganenko*, 2014]. These models are modular in the sense that a magnetopause Chapman-Ferraro current system is derived for each magnetospheric current system, and the complete model field is obtained by adding the magnetic fields of each magnetospheric current system together with its magnetopause shielding field. This approach substantially decreases the mathematical complexity and allows the addition of new current systems without reformulating the entire model. The computational demands of the source-surface method are no longer as substantial relative to conveniently available resources as they once were, so this approach is particularly attractive.

Early models were either static implemented simple parametric deformations of the magnetospheric field consistent with limited observation of the magnetopause shape. The increasing number and distribution

of magnetospheric observations in recent decades improved the characterization of the magnetospheric field substantially. Modern magnetic field models are parameterized by drivers characterizing conditions in the solar wind (e.g., dynamic pressure, interplanetary magnetic field direction and magnitude) and in the magnetosphere (e.g., Kp and Dst indices). Most recent models implement a dynamical data-based modeling approach to represent storm-time magnetic fields with enhanced spatial resolution [*Sitnov et al.*, 2008; *Sitnov et al.*, 2010]. By binning the observations by driving parameters the magnetospheric configuration can be reconstructed empirically [*Stephens et al.*, 2013; *Stephens et al.*, 2016a] and can be used for forecasting by including temporal derivatives of the drivers [*Sitnov et al.*, 2012]. The database of magnetic field observations used to generate the above models is universally useful for developing magnetospheric models. The database is contained in this archive and described in this document. The datasets and data sources are presented in section 2, and data processing is described in section 3. The database format and derivative products are defined in sections 4 and 5.

Datasets and Sources

The original database for magnetic field modeling used to generate input parameters for the TS07 model includes data from Cluster, Geotail, GOES, IMP-8, and Polar and was not publicly available. In the present revision of the dataset includes the original database, which has been augmented with data from Cluster (years 2006-2015), Polar (years 1996 to 2006 and geocentric distances <5 R_E, where R_E is Earth's radius 6371 km), Themis (years 2007-2015), and Van Allen Probes (years 2012-2015). The spin-averaged Cluster data with a temporal resolution of 4 s were obtained from the Cluster Science Archive accessible through the URL http://cosmos.esa.int/web/csa. The data files follow the naming convention C#_CP_FGM_SPIN__????????***.cdf', where "#" and "?" are placeholders for spacecraft identifier and date, respectively. The Polar data with a temporal resolution of 55 s were acquired from the Space Physics Data Facility (SPDF) accessible through the URL ftp://spdf.gsfc.nasa.gov/pub/data/polar. The data files follow the naming convention po_k0_mfe_????????.cdf using the placeholders defined above. The spin-averaged Themis data with a temporal resolution of 3 s were obtained from the Themis data archive accessible through the URL http://themis.ssl.berkeley.edu/data/themis. The data files follow the naming convention th#_l2_fgm_????????.cdf using the placeholders defined above. Finally, the Van Allen Probes data with a sample rate of 64 vectors/s were retrieved from the EMFISIS Science Operations Center accessible through the URL https://emfisis.physics.uiowa.edu. The data file follow the naming convention rbsp-#_magnetometer_hires-gsm_emfisis-L3_????????.cdf using the placeholders defined above.

Data Processing

Modeling of the magnetic field due to magnetospheric current systems requires spatially distributed observations. The general data processing steps are as follows. First, the contributions to the magnetic field from the Earth's internal dynamo, the IGRF model magnetic field was subtracted from the observations after dummy values representing missing or bad data were removed. Since present magnetospheric models consider only the large-scale structure of these currents systems, datasets with high temporal resolution associated with smaller scale structure are not required. Therefore, the observations were averaged in 5-minute intervals centered at the 5-min time steps provided in the database. Position and magnetic field data are represented in Geocentric Solar Magnetospheric (GSM) coordinates, which organize the currents in the magnetosphere. To prevent uncertainties in the IGRF model, which contribute more substantially closer to the surface, to be interpreted as presence of current systems, only data acquired at radial distances >1.5 R_E are included in the database. All averages were

tagged with ancillary solar wind and magnetospheric index data to allow binning of data by the conditions under which they were observed. The solar wind data were taken from the OMNI database available at the SPDF through the URL ftp://spdf.gsfc.nasa.gov/pub/data/omni. These data were propagated in time from the location of observations to the magnetopause. In addition, some dataset specific processing was required and is described below.

Cluster Data Pre-processing

Cluster data processing required removal of spikes in the magnetic field data and removal of poor-quality and solar wind data. The Cluster data showed occasional spikes, which are artefact signals and not physical in nature. These spikes were found to occur in all three components of the magnetic field, B, simultaneously so that their occurrence could be detected by analysis of a single magnetic field component, for which we chose B_z. The occurrence of spikes was detected by computing the temporal derive in B_z and subtracted a 14-point running average from the observations and rejecting data deviating more than 5 nT/s from the running average.

Intervals of poor quality data (e.g., associated with solar eclipses) were previously identified by the Cluster magnetometer team and archived with start and end times in so-called caveats files. These intervals were removed from our dataset.

The Cluster data acquired in the solar wind by removing data points outside the Shue et al. [ref**] magnetopause parameterized by current solar wind condition. Because the 5-min temporal resolution of the modeling database, the approximation of the spacecraft transition into the solar wind using a magnetopause model results in only a small number of solar wind data points being included in the database, which have minimal effect on the magnetospheric configuration, which is typically modeled in a least-squares sense.

Polar Data Pre-processing

Polar data processing required removal of spikes in the magnetic field data and of solar wind data as described for Cluster above.

Themis Data Pre-processing

Themis magnetometer data files do not include the spacecraft position, which is key to magnetic field modeling. The spacecraft position was instead interpolated in time from the spacecraft state files named th#_l1_state_????????.cdf using the notation introduced above. Although the state files also include the eclipse intervals, some eclipse intervals were apparently not recorded in these files. In absence of a complete set of pre-identified intervals, eclipses were identified from geometric condition. For this spacecraft positions within a cylinder of 1 R_E diameter centered on the Earth-Sun line on the planet's nightside. The times of entry into and exit from the eclipse were identified. The identified time intervals were padded with an additional one hour on each side of the eclipse, and the associated data removed from the dataset. Data spike and solar wind data were also removed as described for Cluster above.

Van Allen Problem Data Pre-processing

Unlike for the datasets above, processing of Van Allen Probes magnetic field data required processing of full-time resolution (64 samples per second) data because spike in the magnetic field data were not removed by the instrument team prior to computation of time-averaged derived datasets. The relative amplitudes of the spikes were found to vary between components so that all three components had to be analyzed to identify the bad data point. Because of the high time resolution, the spike removal described for the Cluster dataset was computationally inefficient for the Van Allen Probes data. Fortunately, the spikes in the Van Allen Probes data, which occur at times when the magnetometer changes measurement ranges, consisted of isolated data points, which could be readily identified from first point differences. First-point differences having absolute values larger than 200 nT were eliminated.

In eclipse where the Sun position during satellite spin is not measured, the attitude of the Van Allen Probes spacecraft becomes increasingly inaccurate because booms extending from the spacecraft contract in response to cooler temperatures thus slowing the spin period over time. While this behavior has been successfully modeled in the past, such correction has not been applied to the Van Allen Probes data because there was no requirement to do so. Eclipse periods were identified by the instrument team from spacecraft housekeeping data of the power generated by the solar panels and were eliminated.

The Van Allen Probes did not leave the magnetosphere so that removal of solar wind data was not necessary.

Database Format

The database for magnetic field modeling is stored in American Standard Code for Information Interchange (ASCII) format located in the DATABASE directory. Each file contains data for one satellite and year. The file naming convention is SATELLITE_YEAR_avg_TIM.dat, where SATELLITE is the source, YEAR is the year, and TIM is the averaging time in seconds. For the data processed within this project (Cluster, Polar, Van Allen Probes / RBSP, and THEMIS), the averaging time is 5 min. Data retained from the database of *Tsyganenko and Sitnov* [2007] are 15 min. averages. The format of the file content is listed in Table 1.

Table 1. Database format.

Year	Year of datum
DOY	Day of year of datum
Month	Month of datum
Day	Day of month of datum
Hour	Hour of datum
Minute	Minute of datum
Second	Second of datum
Epoch	CDF epoch time, number of milliseconds since 01-Jan-0000 00:00:00
Count	Number of data point in position and magnetic field average
Position	*X*, *Y*, *Z* position in GSM coordinates in km
Magnetic Field	Dipole-subtracted B_X, B_Y, B_Z components of the magnetic field in GSM coordinates in nT
Magnetic Field Standard Deviation	Standard deviation of dipole-subtracted magnetic field B_X, B_Y, B_Z components in GSM coordinates in nT

Interplanetary Magnetic Field (IMF)	B_X, B_Y, B_Z components of the interplanetary magnetic field in GSM coordinates in nT from OMNI dataset
n_{SW}	Solar wind number density cm^{-3} from OMNI dataset
v_{SW}	Solar wind velocity in km/s from OMNI dataset
AE	AE index (AU-AL) in nT from OMNI dataset
AL Index	AL index innT from OMNI dataset
AU Index	AU index in nT from OMNI dataset
SymH	Symmetric disturbance index for horizontal ground magnetic field component in nT from OMNI dataset
SymH*	Symmetric disturbance index for the horizontal ground magnetic field component correct for solar wind pressure in nT computed as $SymH^* = 0.8\ SymH - 13.0\ (n_{SW}\ v_{SW}^2)^{1/2}$
E_Y	Solar wind dawn-to-dusk electric field in mV/m computed as $-v_X B_Z$ from OMNI dataset
<SymH*>	SymH* average in nT computed using Eq. (2) in *Sitnov et al.* [2012]
<SymH* / dt>	Average temporal derivative of SymH* in nT/h computed using Eq. (3) in *Sitnov et al.* [2012]
$<E_Y>$	E_Y average in mV/m computed using Eq. (1) in *Sitnov et al.* [2012]

The FORTRAN format code for reading the database files is '(i4, 1x, i3.3, 1x, i2.2, 1x, i2.2, 1x, i2.2, 1x, i2.2, 1x, i2.2, 1x, f17.1, 1x, i6, 1x, 3(f14.3,1x), 3(f10.3, 1x), 3(f10.3, 1x), 1x, 13(f10.2, 1x), f10.2)'.

Database Validation and Derivative Products

Validation of the database was, among others, carried out by identification and examination of large discrepancies between the averaged observations and the TS07 model. For this purpose, the TS07 model coefficients were computed in 5 min intervals for the period 1995 to 2016. These coefficients are useful to scientific community and can be found in the "TS07_COEFFICIENTS" directory. The coefficients can be used either with the original FORTRAN code by Tsyganenko and Sitnov available at http://rbspgway.jhuapl.edu/geomag_field/model/index.html or with the IDL Geopack DLM v10 or greater located in the "IDL_GEOPACK_DLM" directory and available at http://ampere.jhuapl.edu/code/idl_geopack.html. A description of the model coefficients is beyond the scope of this document. Limited information on the meaning of the coefficients is provided in the coefficient data files. For details, the reader is referred to *Tsyganenko and Sitnov* [2007].

In addition to the model coefficients, survey plots of the model magnetic field and magnetospheric current distribution were generated in 30 min. intervals for the period 1995 to 2016 and can be found in the directory "SURVEY_PLOTS". An example is shown in Figure 1. Panel (a) shows the time series of the SymH (solid black) and AL (orange) indices in a 5-day window centered on the event time (vertical blue line). The AL index is missing axis labels, which differ from those of the SymH index. The dashed black line represent a six-hour smoothed time series of the SymH index. The remaining panels show (b) the time series of the solar wind dynamic pressure in a 5-day window centered on the event time (vertical blue line); (c) the equatorial distribution of current density in nA/m^2 with current directions within the plane indicated by red arrows; (d) the current distribution same as in (c) with location of magnetic field data included in the model fit indicated by black dots; (e) the equatorial distribution of magnetic field GSM B_Z with data locations same as in (d); (f) the distribution of the GSM *Y* component of the current in nA/m^2 in the noon–

midnight plane (read and blue colors represent currents into and out of the plane, respectively) with magnetic field lines superposed; (g) the current distribution same as (f) with data location superposed; and (h) the pressure distribution in nPa reconstructed from the model. The white circles in panels (c)–(e) and (f) represent geosynchronous orbit while those in panels (f) and (g) are plot artifacts to be ignored.

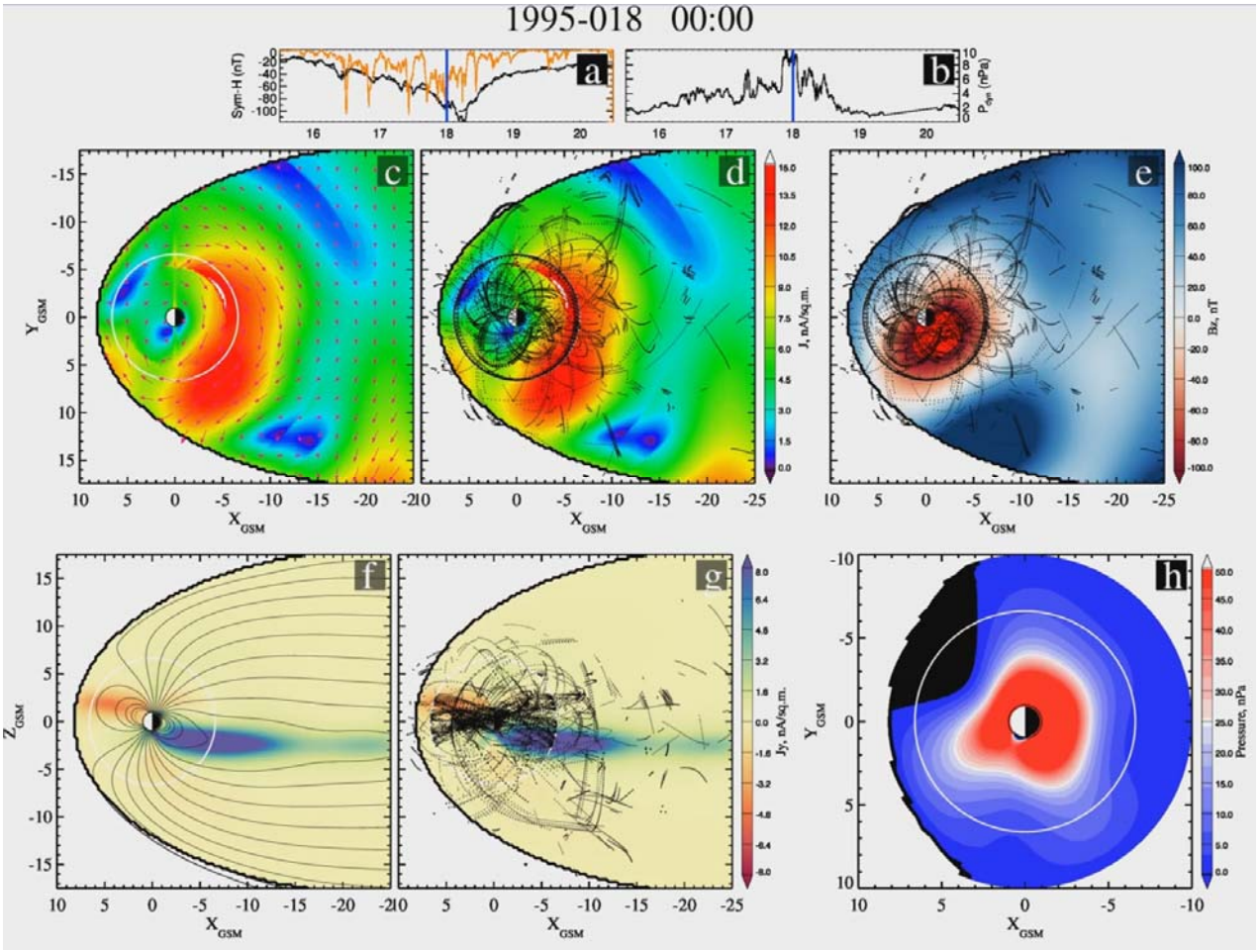

Figure 1. TS07 survey plot for 18 January 1995, 00:00 UTC. See text for description of the panels.

Additional validation of the database was achieved through scientific application of the model coefficients computed using the extended magnetic field database. The improved temporal coverage of the observations during extreme conditions in the magnetosphere was found to allow for higher-fidelity modeling of geomagnetic storms (Stephens et al., 2016b; Sitnov et al., 2017, 2018). For example, for the first time, we were able to resolve the structure of electric currents and plasma pressure distributions the innermost magnetosphere, including eastward and banana currents, as well as the storm-time pressure peaks. We also discovered that the spatial distribution of the observations is now sufficiently high to resolve, for the first time, the three-dimensional structure of the magnetospheric current system associated with magnetic substorms, including the formation of thin current sheets in the growth phase, tail magnetic field depolarization in the expansion phase and the formation of the seed ring current in the late recovery phase (Stephens et al., 2017a,b).

IDL Geopack DLM Software

For validation studies, the TS07 model has been included in the IDL Geopack DLM. The library has long implemented the original FORTRAN releases of the Geopack library and geomagnetic field models (T89, T96, TS04) by Dr. N. A. Tsyganenko, and provides a ready-to-use interface to these codes without requiring knowledge of FORTRAN. The library has been in use by several NASA missions (THEMIS, Van Allen Probes) and NSF facilities (AMPERE, SuperMAG, SuperDARN) and is, for example, an integral part of the THEMIS Data Analysis Software (TDAS now SPEDAS) and the SuperDARN Data Visualization Toolkit (DaViT). In IDL Geopack DLM v10, among others, the routines, GEOPACK_TS07, GEOPACK_TS07_SETPATH, and GEOPACK_TS07_LOADCOEF were added to facilitate computation of the TS07 model field. In addition, the routine GEOPACK_TRACE(_08) has been expanded to trace TS07 model field lines. The IDL Geopack DLM version current at time of archiving is included in the "IDL_GEOPACK_DLM" directory. For the latest version, please check the URL listed above. For use of the new routines, please refer to the documentation provided with the software.

Acknowledgments

This work was supported by NASA grant NNX15AF53G. The Polar satellite magnetic field data were obtained from the NASA Space Physics Data Facility (ftp://spdf.gsfc.nasa.gov/pub/data/polar). The Cluster satellite magnetic field data were obtained from the Cluster Science Archive (http://cosmos.esa.int/web/csa). The THEMIS satellite magnetic field data were obtained through the Themis data archive (http://themis.ssl.berkeley.edu/data/themis). The Van Allen Probes magnetic field data were obtained through the EMFISIS Science Operations Center (https://emfisis.physics.uiowa.edu). The solar wind and IMF data were obtained from the OMNI database (http://omniweb.gsfc.nasa.gov/ow_min.html). The OMNI data files include the SymH index that is offered by the World Data Center for Geomagnetism of Kyoto University (http://wdc.kugi.kyoto-u.ac.jp).

References

Chapman, S., and V. C. A. Ferraro, A new theory of magnetic storms, *Nature*, *126*, 129-130, doi: 10.1038/126129a0, 1930.

Mead, G. D., Deformation of geomagnetic field by the solar wind, *J. Geophys. Res.*, *69*, 1181-1195, doi: 10.1029/Jz069i007p01181, 1964.

Schatten, K. H., J. M. Wilcox, and N. F. Ness, A model of interplanetary and coronal magnetic fields, *Solar Physics*, *6*, 442-455, doi: 10.1007/Bf00146478, 1969.

Schulz, M., and M. C. McNab, Source-Surface Model of the Magnetosphere, *Geophys. Res. Lett.*, *14*, 182-185, doi: 10.1029/Gl014i003p00182, 1987.

Sitnov, M. I., N. A. Tsyganenko, A. Y. Ukhorskiy, and P. C. Brandt, Dynamical data-based modeling of the storm-time geomagnetic field with enhanced spatial resolution, *J. Geophys. Res.*, *113*, A07218, doi: 10.1029/2007ja013003, 2008.

Sitnov, M. I., N. A. Tsyganenko, A. Y. Ukhorskiy, B. J. Anderson, H. Korth, A. T. Y. Lui, and P. C. Brandt, Empirical modeling of a CIR-driven magnetic storm, *J. Geophys. Res.*, *115*, A07231, doi: 10.1029/2009ja015169, 2010.

Sitnov, M. I., A. Y. Ukhorskiy, and G. K. Stephens, Forecasting of global data-binning parameters for high-resolution empirical geomagnetic field models, *Space Weather*, *10*, S09001, doi: 10.1029/2012sw000783, 2012.

Sitnov, M. I., Magnetotail Dynamics, Reporter Review for Division III, IAGA, 27 August – 1 September, Cape Town, South Africa, 2017.

Sitnov, M. I., G. K. Stephens, M. Gkioulidou, V. Merkin, A. Y. Ukhorskiy, H. Korth, P. C. Brandt, N. A. Tsyganenko, Empirical Modeling of Extreme Events: Storm-time Geomagnetic Field, Electric Current, and Pressure Distributions, in Extreme Events in Geospace (N. Buzulukova ed.), 798 pp., doi: 10.1016/B978-0-12-812700-1.00011-X, Elsevier, Amsterdam, 2018.

Stephens, G. K., M. I. Sitnov, J. Kissinger, N. A. Tsyganenko, R. L. McPherron, H. Korth, and B. J. Anderson, Empirical reconstruction of storm time steady magnetospheric convection events, *J. Geophys. Res.*, *118*, 6434-6456, doi: 10.1002/Jgra.50592, 2013.

Stephens, G. K., M. I. Sitnov, A. Y. Ukhorskiy, E. C. Roelof, N. A. Tsyganenko, and G. Le, Empirical modeling of the storm time innermost magnetosphere using Van Allen Probes and THEMIS data: Eastward and banana currents, *J. Geophys. Res.*, *121*, 157-170, doi: 10.1002/2015JA021700, 2016a.

Stephens, G. K., M. I. Sitnov, V. G. Merkin, S. Ukhorskiy, P. C. Brandt, M. Gkioulidou, H. Korth, R. J. Redmon, Storm-time plasma pressure distribution: First results from an advanced empirical geomagnetic field model, Abstract SM32A-06, AGU Fall Meeting, 12-16 Dec., San Francisco, CA, 2016b.

Stephens, G. K., M. I. Sitnov, H. Korth, M. Gkioulidou, A. Y. Ukhorskiy, Global empirical model of substorms derived from spaceborne magnetometer data, 13th International Conference on Substorms, September 25-29, Portsmouth NH, 2017a.

Stephens, G. K., M. I. Sitnov, H. Korth, M. Gkioulidou, S. Ukhorskiy, V. Merkin, Multiscale empirical modeling of the geomagnetic field: From storms to substorms, Abstract SM32B-04, Fall AGU Meeting, 11-15 Dec., New Orleans, LA, 2017b.

Toffoletto, F. R., R. V. Hilmer, T. W. Hill, and G. H. Voigt, Solution of the Chapman-Ferraro problem with an arbitrary magnetopause, *Geophys. Res. Lett.*, *21*, 621-624, doi: 10.1029/94gl00176, 1994.

Tsyganenko, N. A., Modeling the Earth's magnetospheric magnetic feld confined within a realistic magnetopause, *J. Geophys. Res.*, *100*, 5599-5612, doi: 10.1029/94ja03193, 1995.

Tsyganenko, N. A., A model of the near magnetosphere with a dawn-dusk asymmetry - 1. Mathematical structure, *J. Geophys. Res.*, *107*, 1179, doi: 10.1029/2001ja000219, 2002a.

Tsyganenko, N. A., A model of the near magnetosphere with a dawn-dusk asymmetry - 2. Parameterization and fitting to observations, *J. Geophys. Res.*, *107*, 1176, doi: 10.1029/2001ja000220, 2002b.

Tsyganenko, N. A., Data-based modeling of the geomagnetosphere with an IMF-dependent magnetopause, *J. Geophys. Res.*, *119*, 335-354, doi: 10.1002/2013JA019346, 2014.

Tsyganenko, N. A., and M. I. Sitnov, Modeling the dynamics of the inner magnetosphere during strong geomagnetic storms, *J. Geophys. Res.*, *110*, A03208, doi: 10.1029/2004JA010798, 2005.

Tsyganenko, N. A., and M. I. Sitnov, Magnetospheric configurations from a high-resolution data-based magnetic field model, *J. Geophys. Res.*, *112*, doi: 10.1029/2007ja012260, 2007.